Journal of Peptide Science
J. Pept. Sci. 2007; **13**: 575–580
Published online 29 June 2007 in Wiley InterScience (www.interscience.wiley.com). DOI: 10.1002/psc.875

JOURNAL OF PEPTIDE SCIENCE

Temperature-dependent variations of ligand-receptor contact points in hAT_1‡

J. ARSENAULT, M. P. LA HAYE RENAUD, M. CLÉMENT, D. FILLION, G. GUILLEMETTE, R. LEDUC, P. LAVIGNE and E. ESCHER*

Département de pharmacologie, Faculté de Médecine et des Sciences de la Santé, Université de Sherbrooke, 3001, 12ième Avenue Nord, Sherbrooke, Quebec, J1H 5N4, Canada

Received 12 April 2007; Accepted 12 April 2007

Abstract: Photoaffinity labelling is regularly used to investigate proteins, including peptidergic G protein-coupled receptors (GPCR). To this purpose benzophenone photolabels have been widely used to identify many contact residues in ligand-binding pockets. The three-dimensional binding environment of the human angiotensin II type 1 receptor hAT_1 has been determined using an iterative methionine mutagenesis strategy based on the photochemical properties and preferential incorporation of benzophenone onto methionine. This has led to the construction of a ligand-bound receptor structure. The present study investigated the effect of temperature on the accessibility of some of these contact points. The hAT_1 receptor and two representative Met mutants (H256M-hAT_1 and F293M-hAT_1) from the iterative mutagenesis study were photolabelled with the benzophenone-ligand ^{125}I-[Sar^1, Bpa^8]AngII at temperatures ranging from −15 °C to 37 °C. Labelled receptors were partially purified and digested with cyanogen bromide to identify the contact points or segments. There were no changes in receptor contacts or labelling in the 7th transmembrane domains (TMD) of hAT_1 and F293M-hAT_1 across the temperature range. However, a temperature-dependent change in the ligand-receptor contact of H256M-hAT_1 was observed. At −15 °C, H256M labelling was identical to that of hAT_1, indicating that the interaction was specific to the 7th TMD. Significant labelling changes were observed at higher temperatures and at 37 °C labelling occurred almost exclusively at mutated residue H256M-hAT_1 in the 6th TMD. Simultaneous competitive labelling of different areas of this target protein indicated that the ligand-receptor structure became increasingly fluctual at physiological temperatures, while a more compact, low mobility, and low energy conformation prevailed at low temperatures.

Keywords: GPCR; angiotensin II receptor; hAT_1; photoaffinity labelling; ligand contact points; thermodynamics

INTRODUCTION

Over 50% of all pharmaceuticals target G protein-coupled receptors (GPCRs). GPCRs, like many other membrane proteins, are quite refractory to structural characterisation using traditional methods such as nuclear magnetic resonance, electron microscopy, and X-ray crystallography [1–4]. In addition, these methods mainly provide a static picture and thus cannot be used to investigate the microconformational variations within a given protein population that are so crucial to understanding their physiological functions. The need to better understand tertiary structures and the fluctuations inside such proteins is primordial in order to develop a rational approach to designing drugs with the appropriate activities.

Structural analysis by photoaffinity labelling is one of the biochemical methods that has been used for over 40 years to investigate ligand-receptor interactions and the *in situ* localisation of receptors [5–9]. In brief, a biologically relevant ligand containing a photoactivable ligand such as azide, diazirine, or benzophenone is first reversibly bound to its target. Photolysis of the ligand-receptor complex produces a radical intermediate (nitrene, carbene, or keto radical), which forms a covalent bond between the ligand and the receptor [5,9–12]. In the case of receptors, this method has been applied mainly to peptidergic receptors and their ligands, since binding of the photolabile moiety of a peptide causes only minor structural changes to the ligand, thus assuring native-like ligand binding. If sufficient ligand-receptor contact points can be obtained from such receptor labelling experiments, structural elements can be deduced by applying homology modelling approaches to the structural constraints of experimentally determined contact points [13]. In addition, the preferential binding of benzophenone to methionine has been exploited to develop the methionine proximity assay (MPA), an iterative Met-mutagenesis strategy that has been applied to the human angiotensin II type 1 receptor (hAT_1) [14]. Its interaction with angiotensin II (AngII) has been extensively studied in our laboratory [8,13–16]. A key feature of this interaction is the

*Correspondence to: E. Escher, Département de pharmacologie, Faculté de Médecine et des Sciences de la Santé, Université de Sherbrooke, 3001, 12ième Avenue Nord, Sherbrooke, Quebec, J1H 5N4, Canada; e-mail: Emanuel.Escher@USherbrooke.ca
‡This article is published as part of the special issue 2nd International Congress on Natural Peptides to Drugs, April 18–21, 2006, Zermatt, Switzerland.

adoption by the ligand of an extended conformation inside the receptor, with its *C*-terminal residue in close proximity to the 7th transmembrane domain (TMDVII) [15] as well as TMDIII and TMDVI [14,17]. The renin-AngII system is one of the key players in physiological blood pressure control and electrolyte balance where the octapeptide AngII (DRVYIHPF) and its cognate receptor hAT_1 are the principal actors. When AngII binds to hAT_1, a 359-residue GPCR coupled to $G\alpha q_{/11}$, the phospholipase C/inositol phosphate/diacyl glycerol pathways are activated [13,18].

The three-dimensional environment of the *C*-terminal amino acid of the AngII ligand in the receptor-binding pocket, of which 11 receptor residues have been identified to date, was determined using the MPA approach. The ligand-contacting residues of the hAT_1 receptor and the retinal contacting residues in bovine rhodopsin are largely homologous, indicating that their ligand-receptor interactions and structures are very similar [14].

Labelling variability had been observed, but may have been caused by temperature variations. Although, in previous studies, photolabelling was performed on ice, little attempt was made to control the temperature [12,14,16]. The variability may thus have been due to temperature differences. If so, determining the influence of temperature on photolabelling might provide valuable information on receptor conformations and thermodynamics. The goal of the present study was thus to study temperature-dependant changes of labelling patterns. As such, the experimental protocol had to be adapted. The heat intensity of the UV sources was lowered, the convective temperature was precisely controlled over the temperature range used in the experiments, and a multi-sampling capacity was added.

The benzophenone-AngII analogue (^{125}I-[Sar^1, Bpa^8]AngII) used in both the previous and present studies is a competitive antagonist [15,19], alternatively also defined as a neutral orthosteric agonist, that has been used to identify the contact point residues L112M and Y113M in TMDIII, H249M, W253M, H256M, and T260M in TMDVI and 293 through 297 in TMDVII [14–16]. We selected the primary receptor contact mutant F293M-hAT_1 for the present temperature-controlled study. F293M-hAT_1 was identified as the primary photoligand attachment point by Edman degradation of the labelled hAT_1 receptor, which was confirmed using the F293M-hAT_1 mutant [15]. A second mutant (H256M-hAT_1 in TMDVI) with easily identifiable protein fragments was also selected [14]. The native wild-type receptor (WT) hAT_1 was included as a control. The receptors were labelled with ^{125}I-[Sar^1, Bpa^8]AngII at −15, 0, 15, 25, and 37 °C. The labelled receptors were isolated and CNBr-digested to detect changes in labelling patterns.

MATERIALS AND METHODS

Materials

Bovine serum albumin (BSA), bacitracin, soybean trypsin inhibitor, and CNBr were from Sigma-Aldrich (Oakville, ON, Canada), Acetonitrile and ethylene glycol were from Fisher Scientific (Oakville, ON, Canada). Culture media were from Invitrogen (San Diego, CA, USA). FuGene 6 transfection reagent and Protease Inhibitor Cocktail were from Roche Diagnostics (Mannheim, Germany). X-ray films (Kodak BiomaxMS, Rochester, NY, USA) with intensifying screens from Fischer Scientific were used to visualise CNBr digestion fragments.

Synthesis and Radioiodination of the Photoligand

^{125}I-[Sar^1, Bpa^8]AngII was prepared according to Bosse *et al.* [19]. The peptide was iodinated (1500 ± 500 Ci/mmol) as previously described [14,20], except that an acetic acid buffer (pH 5.4) was used.

Cell Cultures and Transfection of COS-7 Cells

COS-7 cells were grown in Dulbecco's modified Eagle's medium (DMEM) supplemented with 2 mM L-glutamine, 10% [v/v] foetal bovine serum, 100 IU/ml penicillin, and 100 μg/ml streptomycin. The cells were incubated at 37 °C in a 5% CO_2 atmosphere and were transfected with plasmids produced during previous studies [14,15] at ∼70% confluence using the FuGene 6 transfection reagent according to the manufacturer's instructions. Thirty-six hours after the initiation of transfection, the cells were washed once with PBS (137 mM NaCl, 0.9 mM $MgCl_2$, 3.5 mM KCl, 0.9 mM $CaCl_2$, 8.7 mM Na_2HPO_4, and 3.5 mM NaH_2PO_4, pH 7.4) and immediately stored at −80 °C until used.

Photoaffinity Labelling

Frozen transfected COS-7 cells were thawed for 1 min at 37 °C. The broken cells were then gently scraped, resuspended in 10 ml of washing buffer (25 mM Tris-HCl [pH 7.4], 100 mM NaCl, and 5 mM $MgCl_2$), and centrifuged (500 *g* for 10 min at 4 °C). The pellet was dispersed in binding buffer (25 mM Tris-HCl [pH 7.4], 100 mM NaCl, 5 mM $MgCl_2$, and 0.1% [w/v] BSA). The broken cell suspension (1 mg of protein) was incubated for 60 min at room temperature in the presence of 3 nM ^{125}I-[Sar^1, Bpa^8]AngII. After centrifugation at 500 *g*, the pelleted broken cells were washed once and resuspended in 0.5 ml of ice-cold washing buffer, then irradiated for 60 min in a temperature-controlled photoreaction chamber (±2 °C) in 5 ml Pyrex eppendorf tubes (Fisher Scientific) immersed in cooling solution (equal parts water and ethylene glycol) within the spiral cage of the UV source (13 W Noma Mini Spiral Black light, λ max 365 nm, serial no. 52-5146-0, Trileaf Distribution, Toronto, ON, Canada). The photoreaction chamber was placed in a temperature-controlled MGW Lauda RC20 Brinkman refrigeration unit equipped with a B. Braun Thermomix II and six UV light sources. The samples were centrifuged (2500 *g* for 10 min at 4 °C) and the pellet was solubilised for 30 min at 4 °C in m-Ripa buffer (50 mM Tris-HCl [pH 8.0], 150 mM NaCl, 0.5% [w/v] deoxycholate, 0.1% [w/v] SDS, and 1% [v/v]

DOI: 10.1002/psc

Nonidet P-40) supplemented with a protease inhibitor cocktail (Complete EDTA-Free) from Roche (Laval, QC, Canada). The cell lysate was centrifuged (15 000 *g* for 25 min at 4 °C) to remove insoluble material and the supernatant was stored at −20 °C until used.

Partial Purification of the Labelled Complex

The solubilised photolabelled receptor complexes were diluted in an equal volume of 2X Laemmli buffer (120 mM Tris-HCl [pH 6.8], 20% [v/v] glycerol, 4% [w/v] SDS, 200 mM DTT, and 0.05% [w/v] bromophenol blue) and incubated for 60 min at 37 °C. SDS-PAGE was performed as previously described [21] using a 10% polyacrylamide preparative gel. The gel was first exposed to an X-ray film with an intensifying screen and was then cut into slices. The radioactive content of the slices was measured using a γ-counter. The labelled receptor was passively eluted from the gel slices into fresh electrophoresis buffer (25 mM Trizma Base [pH 8.3], 250 mM glycine, and 0.1% [w/v] SDS) for 2–3 days at 4 °C with gentle agitation as described by Blanton and Cohen [22]. The eluate (~40 ml) was concentrated to a final volume of 100–250 µl using an Amicon-10 filter from Millipore (Bedford, MA, USA), lyophilised, and dissolved in water in preparation for CNBr digestion.

CNBr Digestion

The partially purified photolabelled receptor (up to 3500 cpm) was diluted in a 3 : 5 mixture of 30% trifluoroacetic acid and 50 mg/ml [w/v] of CNBr in 100% acetonitrile. The 100 µl samples were incubated at room temperature in the dark for 18–24 h. Water (1 ml) was added to terminate the reaction. The samples were lyophilised and dissolved in Tris-tricine with 1X Laemmli buffer, loaded (3500 cpm) on 16.5% SDS-PAGE Tris-tricine running gels from Bio-Rad (Hercules, CA, USA). Photolabelled bands were revealed by autoradiography on X-ray films from Kodak Biomax (Rochester, NY, USA). ^{14}C-labelled low molecular weight protein markers from Amersham Biosciences (Baie d'Urfé, QC, Canada) were used to determine apparent molecular weights. Running conditions and staining procedures were performed according to the manufacturer's instructions.

RESULTS

The results are presented as the means ± SD of at least three independent experiments. Receptor mutants H256M-hAT_1 and F293M-hAT_1 had been characterised previously [14] and their affinities for ^{125}I-[Sar^1, Ile^8]AngII, cell expression rates, and AngII-stimulated IP production were comparable to those of the WT [14].

Photoreaction Time Course

To determine the validity of the photolabelling method used here and to compare it to the previous methods, the efficiency of the temperature-controlled photoreaction chamber used in this study was evaluated. The hAT_1 receptor samples were incubated with ^{125}I-[Sar^1, Bpa^8]AngII at 25 °C, placed in the photoreaction chamber at the selected temperature, and subjected to photolysis. Tubes were removed from the photoreaction chamber at various times to stop the reaction. The samples were analysed by SDS-PAGE and the bands were visualised by autoradiography. Figure 1 shows that the reaction was complete after 60 min of irradiation, confirming that the photolytic capacity of the set-up used in this study was similar to that of the previous study.

Temperature Effects on Photolabelling Yields

The hAT_1 and mutant receptors were incubated with the photoligand for 1 h at 25 °C to allow a binding equilibrium. The photolabelled receptors were then subjected to photolysis at −15 °C or 37 °C. Photoaffinity labelling yields with the WT receptor and both mutant receptors were lower at −15 °C than at 37 °C (Figure 2). Photolabelling at −15 °C resulted in a 2- to 3-fold (2.2 ± 0.8, expressed as labelling ratios

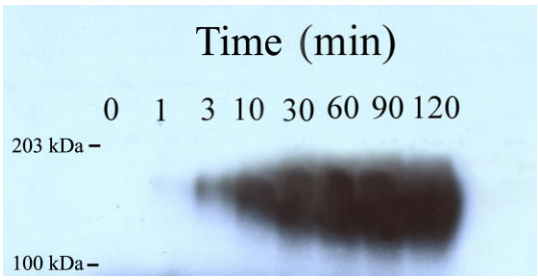

Figure 1 Time-dependant photoreaction at 25 °C. Autoradiography of SDS-PAGE of undigested samples separated on a 10% acrylamide Tris-Glycine gel.

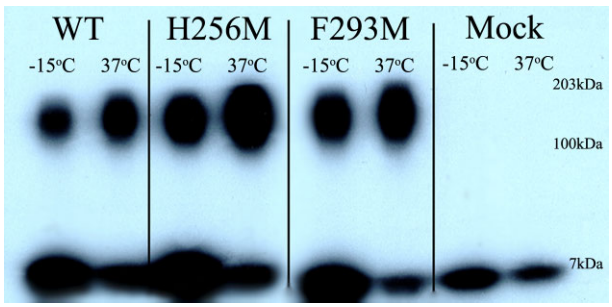

Figure 2 Incorporation yields as a function of temperature. Membranes from hAT_1 WT and mutant receptor (F293M-hAT_1 and H256M-hAT_1) expressing cells, as well as mock transfected cells (empty pcDNA3.1 plasmid), were incubated at 25 °C for 60 min in the dark with a photolabel (16 ± 5 nM ^{125}I-[Sar^1, Bpa^8]AngII). Equal portions were photolabelled for 60 min at −15 °C or 37 °C and then centrifuged. The pellet was resuspended and the fragments were separated by SDS-PAGE on a 10% acrylamide Tris-glycine gel, followed by autoradiography and γ-counting. Labelled receptors migrated between 100 and 203 kDa and unligated ^{125}I-[Sar^1, Bpa^8]AngII] migrated below 6.6 kDa.

DOI: 10.1002/psc

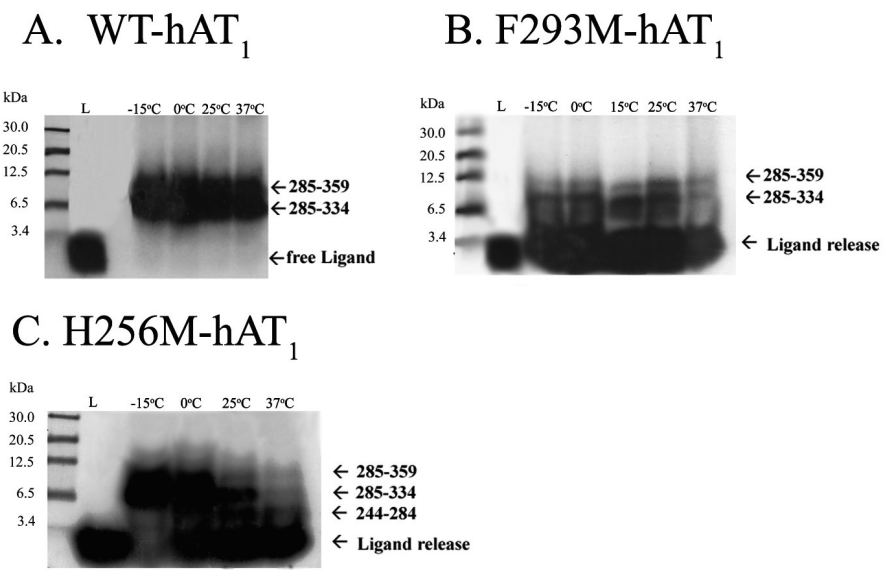

Figure 3 hAT_1 and mutants photolabelled at different temperatures and digested with CNBr. The CNBr fragments were separated by SDS-PAGE on a 16.5% acrylamide Tris-tricine gel followed by autoradiography. Panel (a) WT-hAT_1; panel (b) F293M-hAT_1; and panel (c) H256M-hAT_1. L = free photoligand ^{125}I-[Sar^1, Bpa^8]AngII.

from the γ-counts) lower yield than photolabelling at 37 °C. Photolabelling was also specific to the hAT_1 receptor since no photolabelling occurred in non-hAT_1 expressing cells. Previous studies have also shown that ^{125}I-[Sar^1, Bpa^8]AngII labelling is blocked by an excess of AngII [14,19].

Photolabelling at Different Temperatures and Determining Contact Points

Photolabelling WT-hAT_1 with ^{125}I-[Sar^1, Bpa^8]AngII followed by CNBr digestion gave identical fragments at all the temperatures tested. This result indicated that the interaction, presumably at 293F-hAT_1 and 294N-hAT_1 of TMDVII as has been previously reported [15], did not change (fragment 285–334, Figure 3(a)). In order to confirm that the interaction with residue 293F-hAT_1 of TMDVII was the same at all the temperatures tested, F293M-hAT_1 was labelled and processed using the same conditions. CNBr digestion of the intact, prepurified ligand-receptor complex (100–203 kDa) produced, in addition to small amounts of the fragments mentioned above, a major fragment (<3.4 kDa) that had the same electrophoretic mobility as the free ligand [14,15]. This CNBr digestion profile indicated that the methionine residue inserted at position 293F-hAT_1 of the receptor was labelled at all the temperatures tested (Figure 3(b)). Mutant H256M-hAT_1, on the other hand, had a much different profile. At −15 °C, essentially the same fragments as those of the WT receptor (7.2 kDa fragment 285–334 and the partially digested 10.0 kDa fragment 285–359) were labelled, indicating that an interaction identical to that with WT-hAT_1 had occurred with the TMDVII of mutant H256M-hAT_1. At higher temperatures, however, the labelling of H256M-hAT_1 increasingly shifted to other fragments. At 37 °C, CNBr digestion largely produced a single fragment that co-migrated with the free ligand (Figure 3(c)). This fragment corresponded to CNBr-induced ligand release but, in this mutant, the methionine inserted into TMDVI of H256M-hAT_1 was labelled (Figure 3(c)). At intermediate temperatures, a mixture of both labelling patterns was observed, with TMDVI-labelling increasing in parallel with temperature. In addition, a 5.8-kDa fragment appeared that was compatible with fragment 244–284 in TMDVI of the third extracellular loop. This fragment may have been a result of partial cleavage of the labelled methionine. Figure 4 is a schematic of the regions quantified in the SDS-PAGE gels.

DISCUSSION

Functional proteins of homoeothermic organisms are more active at physiological temperatures. This is due in large part to the fact that chemical reactions and the conformation of structural isoforms are optimal at 37 °C. At cold or sub-zero conditions, most physiological processes cease as well as the individual biochemical reactions. However, many studies are carried out at low temperatures in order to investigate the conformations of proteins. Thermodynamic studies have played a pivotal role in understanding the functions of proteins in general [23,24] and soluble proteins in particular [25], as well as membrane protein interactions [26].

Previous MPA studies on hAT_1 and N111G-hAT_1 at 0 °C revealed that these proteins have 11 and 10 contact points, respectively [14,27]. The contact

DOI: 10.1002/psc

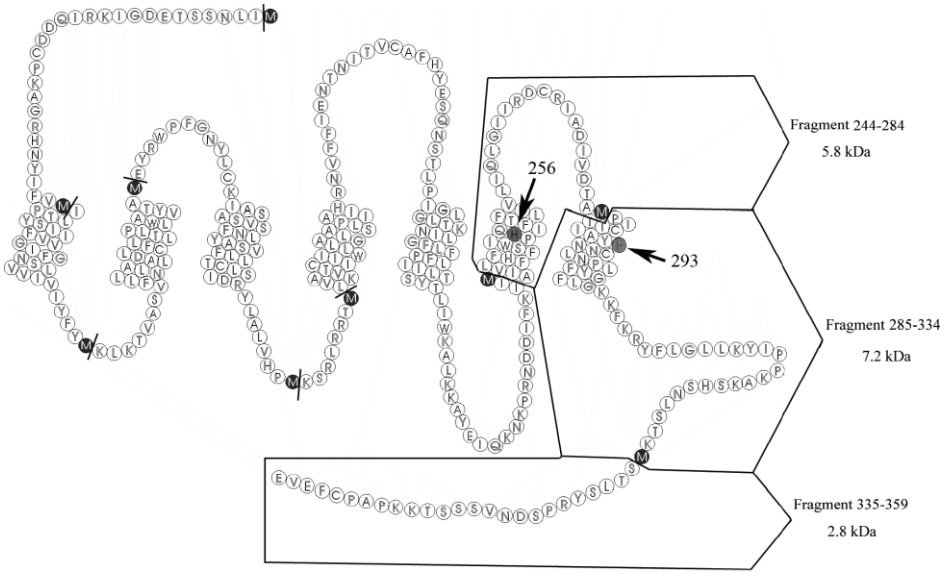

Figure 4 Schematic representation of the possible fragment sizes obtained by CNBr digestion after photo-incorporation of the radioactive ligand into the receptor. The CNBr cleavage sites, the native methionines, and the inserted methionines (H256M-hAT$_1$ and F293M-hAT$_1$) are indicated in black.

points must have a certain conformational mobility since they are necessarily outside the strict Van der Waals radius of the photolabile moiety [28]. The present study showed, especially with the F293M-hAT$_1$ mutant, that the contact points and conformations observed at low temperatures were also present at physiological temperatures since photolabelling this mutant produced the same CNBr fragments as the wild-type in addition to methionine labelled ligand release, indicating that accessibility of the photolabelling moiety to the receptor residue F293M-hAT$_1$ had not changed. However, while photolabelling H256M-hAT$_1$ at $-15\,^{\circ}$C produced a pattern identical to that of WT-hAT$_1$, as the temperature was increased, a progressive shift to labelling of the methionine residue inserted at H256M-hAT$_1$ on TMDVI was observed. The photogenerated benzophenone radical in Bpa preferentially binds to methionine, with a reaction rate 10^4 times that with alanine [29]. However, to be labelled, the methionine residue must be accessible to the benzophenone radical. From our observations at $-15\,^{\circ}$C, the methionine at position H256M-hAT$_1$ was not accessible because the labelling took place almost exclusively on the non-Met residues 293F-hAT$_1$ and 294N-hAT$_1$ in TMDVII [15]. TMDVI and, in particular residue H256M-hAT$_1$, became increasingly accessible with increasing temperature and, at $37\,^{\circ}$C, labelling occurred almost exclusively on the inserted methionine. This does not mean that this residue becomes the exclusive contact point at physiological temperatures but merely reflects the strong selectivity of the photolabel for methionine. For example, labelling still occurred on TMDVII of WT-hAT$_1$ and the F293M-hAT$_1$ mutant at $37\,^{\circ}$C. This indicates that while residue H256M-hAT$_1$ became increasingly accessible, the 293F-hAT$_1$ residu remained constantly accessible. A temperature-induced ligand-receptor dynamic process thus permits translational movements [30] that allow methionine-tagging to occur, favouring the lower activation energy of the labelling reaction. The possibility that the behaviour of the H256M-hAT$_1$ mutant may be due to a simple perturbation of the hAT$_1$ structure through the H to M mutation [31,32] is unlikely since the pharmacological activities of WT-hAT$_1$ and the two mutants are highly similar [14].

Photochemical activation of the benzophenone moiety and triplet radical decay rates remained virtually unchanged in the $-15\,^{\circ}$C to $37\,^{\circ}$C temperature range. The increase in photolabelling yields at higher temperatures was thus more likely a reflection of intra-receptor ligand mobility and increased collision rates leading to appropriate C–H bonds than of an increase in the photochemical activation rate.

In conclusion, our results show that at physiological temperatures a signal transduction protein like hAT$_1$ GPCR should not be seen as a protein that is confined to a minimum energy conformation but rather as a structure that allows access to several conformational populations that could be required to exert its physiological functions, including ligand binding and G protein-signalling. Since the number of possible intermediate conformations is unknown [25,33], further studies are required to get a better picture of how hAT$_1$ functions. MPA studies are currently underway to investigate the potential ligand accessibilities of most residues in the seven TMDs of hAT$_1$ and other peptidergic receptors as well as their constitutively

DOI: 10.1002/psc

active mutants (CAMs). Comparisons of contact points in WT and CAM receptors may also provide insights into the conformational changes that occur during receptor activation.

Acknowledgements

We would like to thank the CIHR and CHSFQ for funding this research and Marie-Reine Lefebvre and Brian Holleran for their help and technical support. M.C. has a studentship from HSFC. R.L. is a career investigator and P.L. is a senior scholar of the *Fond le la Recherche en Santé du Québec.* E.E. is the recipient of the J.C. Edwards Chair in Cardiovascular Research.

REFERENCES

1. Unwin PN, Henderson R. Molecular structure determination by electron microscopy of unstained crystalline specimens. *J. Mol. Biol.* 1975; **94**: 425–440.
2. Jastrzebska B, Fotiadis D, Jang GF, Stenkamp RE, Engel A, Palczewski K. Functional and structural characterization of rhodopsin oligomers. *J. Biol. Chem.* 2006; **281**: 11917–11922.
3. Wess J. G-protein-coupled receptors: molecular mechanisms involved in receptor activation and selectivity of G-protein recognition. *FASEB J.* 1997; **11**: 346–354.
4. Matthews EE, Zoonens M, Engelman DM. Dynamic helix interactions in transmembrane signaling. *Cell* 2006; **127**: 447–450.
5. Ruoho AE, Kiefer H, Roeder PE, Singer SJ. The mechanism of photoaffinity labeling. *Proc. Natl. Acad. Sci. U.S.A.* 1973; **70**: 2567–2571.
6. Lifter J, Hew CL, Yoshioka M, Richards FF, Konigsberg WH. Affinity-labeled peptides obtained from the combining region of myeloma protein 460. I. Heavy-chain-labeling patterns using dinitrophenyl azide photoaffinity label. *Biochemistry* 1974; **13**: 3567–3571.
7. Battersby MK, Richards JG, Mohler H. Benzodiazepine receptor: photoaffinity labeling and localization. *Eur. J. Pharmacol.* 1979; **57**: 277–278.
8. Escher E, Nguyen TM, Regoli D. Photoaffinity labeling of the angiotensin II receptor; pharmacology of the labeling peptides in the dark. *Can. J. Physiol. Pharmacol.* 1978; **56**: 956–962.
9. Hesse L, Erdmann G, Eschenhagen T, Wellhoner HH. Improved method for autoradiographic localization of beta-adrenoceptors using photoaffinity labelling. *Naunyn Schmiedebergs Arch. Pharmacol.* 1993; **347**: 494–499.
10. Singh A, Thornton ER, Westheimer FH. The photolysis of diazoacetylchymotrypsin. *J. Biol. Chem.* 1962; **237**: 3006–3008.
11. Dorman G, Prestwich GD. Benzophenone photophores in biochemistry. *Biochemistry* 1994; **33**: 5661–5673.
12. Fillion D, Deraet M, Holleran BJ, Escher E. Stereospecific synthesis of a carbene-generating angiotensin II analogue for comparative photoaffinity labeling: improved incorporation and absence of methionine selectivity. *J. Med. Chem.* 2006; **49**: 2200–2209.
13. Boucard AA, Wilkes BC, Laporte SA, Escher E, Guillemette G, Leduc R. Photolabeling identifies position 172 of the human AT(1) receptor as a ligand contact point: receptor-bound angiotensin II adopts an extended structure. *Biochemistry* 2000; **39**: 9662–9670.
14. Clement M, Martin SS, Beaulieu ME, Chamberland C, Lavigne P, Leduc R, Guillemette G, Escher E. Determining the environment of the ligand binding pocket of the human angiotensin II type I (hAT1) receptor using the methionine proximity assay. *J. Biol. Chem.* 2005; **280**: 27121–27129.
15. Perodin J, Deraet M, Auger-Messier M, Boucard AA, Rihakova L, Beaulieu ME, Lavigne P, Parent JL, Guillemette G, Leduc R, Escher E. Residues 293 and 294 are ligand contact points of the human angiotensin type 1 receptor. *Biochemistry* 2002; **41**: 14348–14356.
16. Rihakova L, Deraet M, Auger-Messier M, Perodin J, Boucard AA, Guillemette G, Leduc R, Lavigne P, Escher E. Methionine proximity assay, a novel method for exploring peptide ligand-receptor interaction. *J. Recept. Signal Transduct. Res.* 2002; **22**: 297–313.
17. Gagnon T, Fillion D, Lefebvre MR, Escher E. Synthesis of an agonistic, difluoro-azido photolabel of angiotensin II and labeling of the AT1 receptor: transmembrane domains 3, 6, and 7 form the ligand-binding pocket. *J. Recept. Signal Transduct. Res.* 2006; **26**: 435–451.
18. Auger-Messier M, Arguin G, Chaloux B, Leduc R, Escher E, Guillemette G. Down-regulation of inositol 1,4,5-trisphosphate receptor in cells stably expressing the constitutively active angiotensin II N111G-AT(1) receptor. *J. Mol. Endocrinol.* 2004; **18**: 2967–2980.
19. Bosse R, Servant G, Zhou LM, Boulay G, Guillemette G, Escher E. Sar1-p-benzoylphenylalanine-angiotensin, a new photoaffinity probe for selective labeling of the type 2 angiotensin receptor. *Regul. Pept.* 1993; **44**: 215–223.
20. Fraker PJ, Speck JC Jr Protein and cell membrane iodinations with a sparingly soluble chloroamide, 1,3,4,6-tetrachloro-3a, 6a-diphrenylglycoluril. *Biochem. Biophys. Res. Commun.* 1978; **80**: 849–857.
21. Laemmli UK. Cleavage of structural proteins during the assembly of the head of bacteriophage T4. *Nature* 1970; **227**: 680–685.
22. Blanton MP, Cohen JB. Identifying the lipid-protein interface of the Torpedo nicotinic acetylcholine receptor: secondary structure implications. *Biochemistry* 1994; **33**: 2859–2872.
23. Bains G, Freire E. Calorimetric determination of cooperative interactions in high affinity binding processes. *Anal. Biochem.* 1991; **192**: 203–206.
24. Freire E. Structural thermodynamics: prediction of protein stability and protein binding affinities. *Arch. Biochem. Biophys.* 1993; **303**: 181–184.
25. Xie D, Freire E. Structure based prediction of protein folding intermediates. *J. Mol. Biol.* 1994; **242**: 62–80.
26. Freire E, Biltonen R. Estimation of molecular averages and equilibrium fluctuations in lipid bilayer systems from the excess heat capacity function. *Biochim. Biophys. Acta* 1978; **514**: 54–68.
27. Clement M, Chamberland C, Perodin J, Leduc R, Guillemette G, Escher E. The active and the inactive form of the hAT1 receptor have an identical ligand-binding environment: an MPA study on a constitutively active angiotensin II receptor mutant. *J. Recept. Signal Transduct. Res.* 2006; **26**: 417–433.
28. Saviano M, Improta R, Benedetti E, Carrozzini B, Cascarano GL, Didierjean C, Toniolo C, Crisma M. Benzophenone photophore flexibility and proximity: molecular and crystal-state structure of a Bpa-containing trichogin dodecapeptide analogue. *Chembiochem* 2004; **5**: 541–544.
29. Marciniak BB, Bobrowski K, Hug GL. Quenching of triplet states of aromatic ketones by sulfur-containing amino acids in solution. Evidence for electron transfer. *J. Am. Chem. Soc.* 1993; **97**: 11937–11943.
30. Murphy KP, Xie D, Thompson KS, Amzel LM, Freire E. Entropy in biological binding processes: estimation of translational entropy loss. *Proteins* 1994; **18**: 63–67.
31. Schwartz TW, Perlman S, Rosenkilde MM, Hjorth SA. How receptor mutagenesis may confirm or confuse receptor classification. *Ann. N. Y. Acad. Sci.* 1997; **812**: 71–84.
32. Munson M, Balasubramanian S, Fleming KG, Nagi AD, O'Brien R, Sturtevant JM, Regan L. What makes a protein a protein? Hydrophobic core designs that specify stability and structural properties. *Protein Sci.* 1996; **5**: 1584–1593.
33. Kenakin T. Agonist-specific receptor conformations. *Trends Pharmacol. Sci.* 1997; **18**: 416–417.